Adsorption of Adenine and Thymine and Their Radicals on Single-Wall Carbon Nanotubes

ARTICLE *in* THE JOURNAL OF PHYSICAL CHEMISTRY C · DECEMBER 2007

Impact Factor: 4.77 · DOI: 10.1021/jp074270g

3 AUTHORS:

Yaroslav Shtogun
University of South Florida
17 PUBLICATIONS **241** CITATIONS
SEE PROFILE

Lilia M. Woods
University of South Florida
104 PUBLICATIONS **1,200** CITATIONS
SEE PROFILE

Galina Dovbeshko
Institute of Physics of the National Academy …
95 PUBLICATIONS **747** CITATIONS
SEE PROFILE

Adsorption of Adenine and Thymine and Their Radicals on Single-Wall Carbon Nanotubes

Yaroslav V. Shtogun,*,† Lilia M. Woods,† and Galina I. Dovbeshko‡

Department of Physics, University of South Florida, Tampa, Florida 33620, and Department of Physics of Biological Systems, Institute of Physics, National Academy of Sciences of Ukraine, Prospect Nauki 46, Kiev, Ukraine 03028

Received: June 1, 2007; In Final Form: September 17, 2007

The adsorption of adenine, thymine, and their radicals on the surfaces of metallic and semiconducting single-wall carbon nanotubes are studied by local density approximation within density functional theory. The energies and equilibrium distances for several configurations are obtained after relaxation of the entire system. The changes of the molecular bonds and angles before and after adsorption are also calculated. We find that all molecules are physisorbed due to the interaction of their π-orbitals and the π-orbitals of the nanotubes. The electronic structure of both metallic and semiconducting nanotubes is not changed significantly upon adsorption, and thus only small changes in the carbon nanotube properties are expected. The results from these studies can be used as a model of DNA interaction with the surfaces of carbon nanotubes.

1. Introduction

Carbon nanotubes have been shown to have unique electronic, thermal, optical, mechanical, and transport properties, which play a crucial role in their integration into nanotechnological devices.[1−3] Their interaction properties with other compounds are the main element in many applications involving carbon nanotubes such as gas storage, sensors, biocompatible agents, functionalized elements, and more. In particular, the adsorption of polymers, organic molecules, proteins, and DNA on carbon nanotube surfaces has attracted considerable attention recently due to the potential applications in physics, chemistry, biology, and materials science.

It has been demonstrated that carbon nanotube noncovalent functionalization with aromatic and organic molecules[4,5] as well as carbon nanotube sensors for some aromatics[6,7] can be achieved. In addition, significant attention has been paid to DNA/carbon nanotube complexes which have been shown to be suitable for DNA conformation transformation,[8,9] DNA hybridization,[10] electrochemical detection of DNA,[11] DNA encapsulation,[12] and DNA sensors.[13,14] Several studies have been carried out on DNA wrapped around carbon nanotubes and sorting the nanotubes by diameter and chirality as well as DNA sequencing by electronic methods.[15−17] Other applications of DNA/carbon nanotube complexes related to antitumor drug delivery systems, enzyme immobilization, and DNA transfection have also been envisioned.[18] Thus these achievements demonstrate the versatility and promise of DNA/carbon nanotube structures and they warrant the need for fundamental understanding of the nature and important factors of the DNA/carbon nanotube interactions.

DNA is an important element of the living cell that contains genomic information. It is a large quasi-one-dimensional structure consisting of two polynucleotide chains. Each chain consists of random repetition of nucleotides which are connected to each other through hydrogen bonds. Each nucleotide has a phosphate group linked to a sugar ring and a base molecule also connected to the sugar ring.[19] The bases are the purines comprised by adenine (A) and guanine (G), and the pyrimidines comprised by thymine (T) and cytosine (C). The stability of the DNA molecule is governed by the hydrogen bonds between the purines and pyrimidines (two hydrogen bonds for A-T and three for G-C), the π-stacking of the bases, and the screening of the negative charges carried by the phosphate groups on its backbone.[19]

We examine in more detail the structure of the DNA bases. This is motivated by the fact that our study will be centered at understanding of how the bases interact with carbon nanotubes. The purines (A and G) are nitrogenous molecules consisting of one six-member pyrimidine ring and one five-member imidazole ring with an NH_2 functional group for A and an NH_2 and CO groups for G. The pyrimidines (T and C) are nitrogenous bases consisting of one six-member pyrimidine ring with a CH_3 and CO groups for T and an NH_2 and CO groups for C. Thus, purines and pyrimidines have a common structural feature from the π-orbitals perpendicular to the molecular plane, but the functional groups provide their different electron affinities. The DNA bases are also stable structures by themselves, and they are often considered in adsorption studies as a prototype of the DNA interaction with other compounds. For example, studies of DNA bases interacting with semiconducting[20] and metallic surfaces[21,22] have been carried out in order to gain knowledge of the mechanisms governing the adsorption of DNA building blocks on nonorganic materials.

Graphite and semiconducting and metallic carbon nanotubes, similar to the purines and pyramidines, have delocalized π-orbitals perpendicular to the surface. Therefore, the DNA bases/carbon nanotube systems can be viewed as two interacting nitrogenous and carbon π-systems. The $\pi-\pi$ interaction is long-ranged and relatively weak. It leads to stacking which is apparent in the interlayer bonding in graphite,[23] between the bases in the DNA molecule,[24] or in aromatic−carbon nanotube complexes.[25,26]

The focus of this study is to investigate the adsorption of two DNA bases on single-wall carbon nanotube (SWNT)

* Corresponding author. E-mail: yshtogun@cas.usf.edu.
† University of South Florida.
‡ Institute of Physics, Ukrainian Academy of Science.

10.1021/jp074270g CCC: $37.00
Published on Web 11/15/2007

surfaces by using first-principle calculations based on density functional theory (DFT). These are adenine as a model for purines/SWNT interaction and thymine as a model for pyrimidines/SWNT interaction. Also, to understand the response of both metallic and semiconducting SWNT, we study the adsorption of adenine on the metallic (6,6) SWNT and the adsorption of thymine on the semiconducting (8,0) SWNT.

In addition to the A/SWNT and T/SWNT, we consider the adsorption of adenine and thymine radicals on the same SWNT. Experimental work has shown that all ionizing radiation exposures induce mutagenic and recombinogenic lesions in DNA which are linked to strand breaks, base damage, and clustered damage.[27] In particular, damage mechanisms to DNA bases have been related to creation of base radicals[28,29] as well as tautomers of bases.[30] Here, we consider the adsorption of radicals, obtained by deprotonation which is removing a hydrogen (H) atom from the base,[31,32] in order to provide a model of how damaged DNA might interact with carbon nanotube surfaces.

The paper is organized as follows. In section 2, the method for the calculations is described. In section 3, we give results from these calculations. Section 4 contains the conclusions.

2. Method of Calculation

The results presented in this work are obtained by self-consistent DFT calculations within the Vienna Ab Initio Simulation Package (VASP).[33] This code uses a plane wave basis and a periodic supercell method. It utilizes either ultrasoft Vanderbilt pseudopotentials or a projector-augmented wave method to account for the core electrons.[34] These methods require a relatively small number of plane waves per atoms, are scalable for large systems, and are chemically accurate. For the systems studied here with a full valence shell (A and T), nonspin-polarized calculations were performed. For the A and T radicals that have partially filled valence shells due to the deprotonation, results from spin-polarized calculations are presented.

DFT is most successful in describing short-ranged strong chemical forces, but it gives an imperfect quantitative description for long-range weak interactions, as the local density approximation (LDA) for the exchange-correlation functional tends to overestimate the adsorption energy and the generalized gradient approximation (GGA) tends to underestimate it.[23] All electron quantum mechanical calculations of the real many-body wave function including higher-order corrections to the Hartree-Fock method should give an accurate description of the missing from DFT long-ranged dispersion forces,[35] but this method cannot manage large and extended systems. Nevertheless, DFT-LDA has been found to give a useful model for large graphitic structures providing a distance between layers matching the one from experiment and the corrugation parallel to a graphite layer or along a nanotube.[35−39] Also DFT gives an accurate description of the electronic structure along the planes of graphite and along the axis of the carbon nanotube, for which the electronic structure is determined by the sp^2 orbitals and the van der Waals contribution is not significant. Other studies have used DFT in combination with semiempirical potentials for the interlayer interaction to improve the interaction energy, but the relative orientation, distance, and electronic structure are only slightly different from the DFT results.[40] On the basis of the past success of DFT to describe the equilibrium distances, corrugation, and electronic structure of graphitic compounds, we adopt it as a model for describing the adsorption of the A and T bases and their radicals on SWNT. Therefore, we use DFT to establish an initial understanding of the relevant factors for the adsorption configurations, corrugation, and electronic structure of DNA bases/SWNT complexes.

The adsorption of adenine on the metallic SWNT (6,6) and the adsorption of thymine on the semiconducting (8,0) SWNT is considered with nonspin-polarized LDA. These are closed valence shell structures. Spin-polarized calculations are done for the adsorption of the partially filled valence shell A-radical on (6,6) SWNT and T-radical on (8,0) SWNT.

The bare nanotubes are fully relaxed initially obtaining an optimized length of 12.25 Å for the (6,6) SWNT, which corresponds to 5 unit cells along the tube axis, and an optimized length of 17.03 Å for the (8,0) SWNT, which corresponds to 4 unit cells along the tube axis. The lateral sizes of both supercells are 22.04 and 22.12 Å for the (6,6) and (8,0) SWNT, respectively, in order to avoid interactions between tubes from adjacent unit cells. A $1 \times 1 \times 7$ Monhkorst-Pack k grid for sampling the Brillouin zone is taken. The cutoff energy is taken to be 420 eV. The energy convergence criterion is 10^{-5} eV, and the force convergence criterion is 0.005 eV/Å. During the adsorption calculations, the entire system is allowed to relax in each case. For all molecules, the adsorption energy is calculated using the following relationship:

$$E_{ads} = E_{mol} + E_{SWNT} - E_{mol/SWNT}$$

where E_{mol} is the total energy for the relaxed molecule only, E_{SWNT} is the total energy for the relaxed pristine SWNT, and $E_{mol/SWNT}$ is the total energy of the relaxed molecule/SWNT structure.

3. Results

3.1. Adsorption Configurations, Equilibrium Distances, and Energies. Some reports have been published on the adsorption of DNA fragments on graphite and carbon nanotubes. For example, the adsorption of adenine on graphite has been investigated by scanning tunneling microscopy (STM),[41] by noncontact atom force microscopy,[42] and by thermal desorption spectroscopy.[43] These works report equilibrium distances ranging from 3.3 to 3.57 Å. Thymine adsorbed on graphite has also been studied by STM.[44,45] The adsorption energy of adenine on graphite has also been calculated using DFT-LDA, DFT-GGA, and DFT-GGA with an empirical correction for the van der Waals forces.[46] It was shown that the LDA energy is 0.46 eV and the equilibrium distance is 3.1 Å, the GGA with the semiempirical London[40] correction energy is 1. 09 eV and the equilibrium distance is 3.4 Å, and the GGA energy is 0.07 eV with a distance of 4.0 Å. In all cases the main contribution to the energy comes from exchange-correlation. The electronic structure in terms of adsorption configurations, energy bands, and density of states was not investigated in that reference. In ref 47, the interaction of a nucleoside, which consists of DNA bases and a deoxyribose sugar ring with a semiconducting (10,0) carbon nanotube using DFT-LDA results gives similar adsorption energies (0.43−0.46 eV) as in the case of the adenine/graphite system. In that reference, other possible potential minima were found, but no details of relevant energies and distances were given. Also the interaction between a DNA with eleven base pairs using DFT with Tight Binding scheme for an array of finite length nanotubes was considered. It was shown that the band gap of such an array of DNA/nanotubes can be decreased.[48]

Our investigations build on the results obtained in those references. By considering one of the smallest building DNA

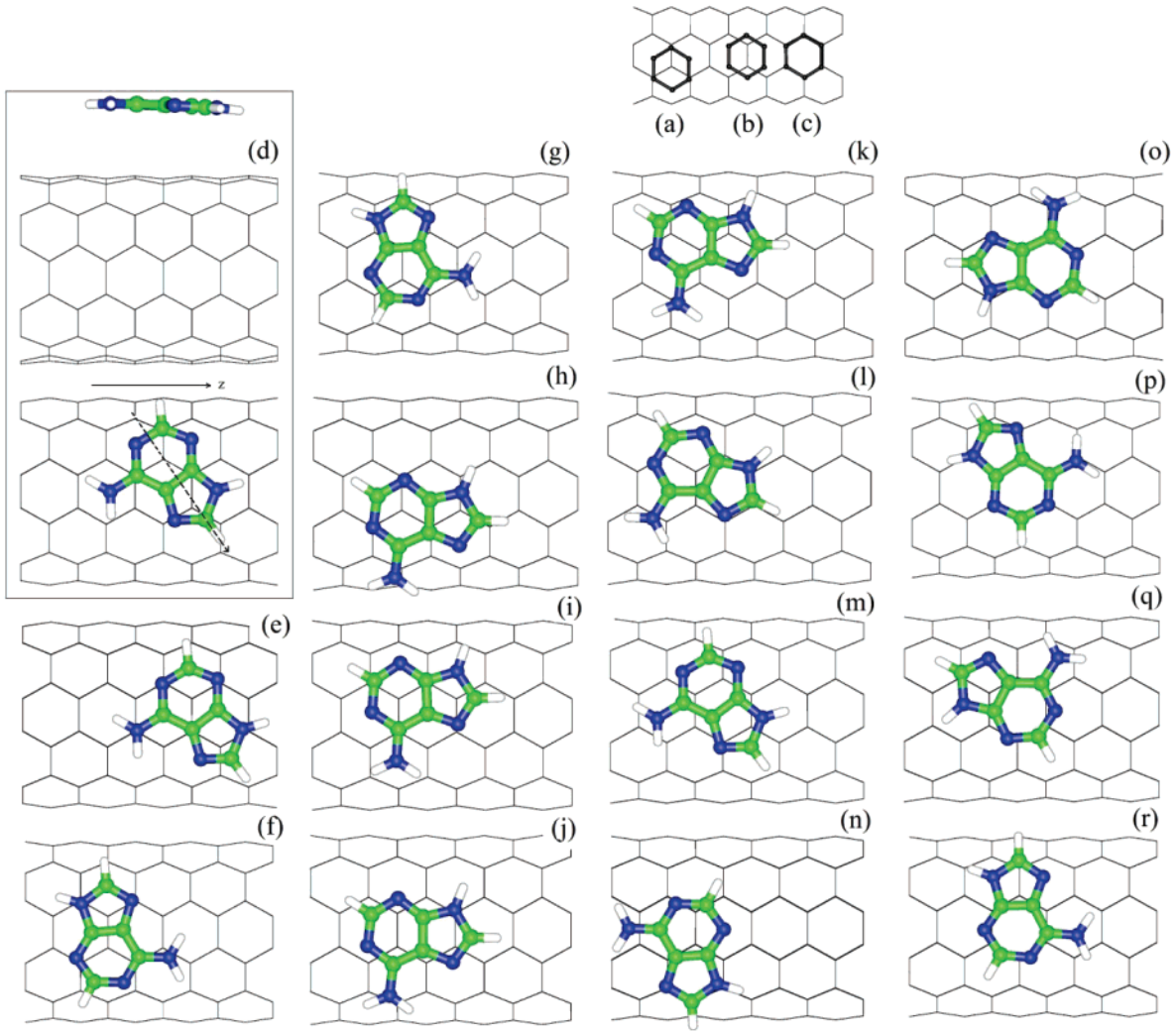

Figure 1. The symmetry adsorption sites of a hexagonal ring structure: (a) top symmetry site, (b) bridge symmetry site, and (c) hollow symmetry site. Adsorption configurations of adenine on the (6,6) SWNT surface: (d) Top_60b configuration with front and top views (the most stable configuration), (e) Top_60a, (f) Top_90a, (g) Top_90b, (h) Top_a, (i) Top_b, (j) Bridge_a, (k) Bridge_b, (l) Bridge_30, (m) Bridge_60, (n) Bridge_90, (o) Hollow, (p) Hollow_30, (q) Hollow_60, (r) Hollow_90. The numbers 30, 60, and 90 represent relative angles between the longitudinal axis of adenine (dashed line) and the *z*-direction of the nanotube.

blocks, our results help determine the dominant contribution in larger DNA fragments.[47,48] We examine in detail the different adsorption configurations, equilibrium distances, and electronic structure for the DNA bases/SWNT and DNA base radicals/SWNT systems and provide analysis of the factors influencing the adsorption process. The DFT-LDA approach is a reasonable model for this goal, which is indicated by the review of the published work on graphitic structures adsorption earlier[41−45] as well as our own experience.[39]

Several positions of the adenine and thymine molecules on the SWNT surfaces were investigated. There are three distinct symmetry sites related to the relative position of the hexagonal ring in each molecule with respect to the nanotube carbon rings. These sites are top (Figure 1a), bridge (Figure 1b), and hollow (Figure 1c), and they have been determined and investigated for the adsorption of benzene and simple benzene derivatives on carbon nanotubes previously.[37−39] In addition, adenine is an extended molecule due to the five-member ring attached to its hexagonal ring. As a result, there are many more possible configurations as compared to those for a molecule with just a hexagonal ring.[37−39]

We considered fifteen locations of adenine on the (6,6) SWNT, and they are shown on Figure 1 after relaxation of the entire system. Figure 1d shows the most stable configuration after adsorption—Top_60b, where the adenine is in the top symmetry site and the axis of the molecule is at about 60° with respect to the nanotube axis. The N atom from the NH_2 group is in top position while the two H atoms are above the two C atoms from the nanotube. Thymine has only one hexagonal ring with a methyl functional group. We consider five configurations on the (8,0) SWNT surface, see Figure 2 (shown after relaxation of the structure). The most stable one is near the top symmetry site, see Figure 2a, where the hexagonal ring and the C atom from the CH_3 group are also in top location. Thymine is slightly tilted with the oxygen opposite to the CH_3 group closer to the nanotube axis.

For the A-radical, we take the most stable configuration for A/SWNT (Top_60b). There are several A-radicals that one can obtain if a H atom is removed.[31] We take only this deprotonated radical for which the H atom from the NH_2 (N6 atom) group has been removed, see Figure 3. This radical has the second largest most stable energy as compared to the one for which H from N9 is removed, but since N9 in adenine is connected to a DNA sugar ring, such a radical is much more difficult to create when adenine is part of the whole DNA molecule.[31] Figure 3a shows the A-radical/SWNT configuration after relaxation. For

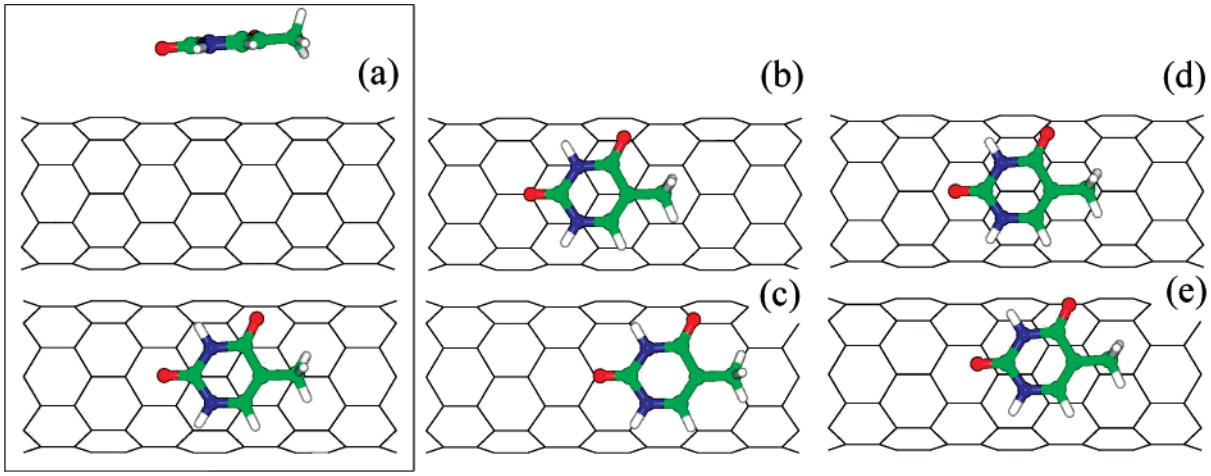

Figure 2. Equilibrium configurations of thymine adsorbed on (8,0) SWNT: (a) Top_a configuration with front and top views (most stable configuration), (b) Top_b, (c) Hollow, (d) Bridge_a, (e) Bridge_b.

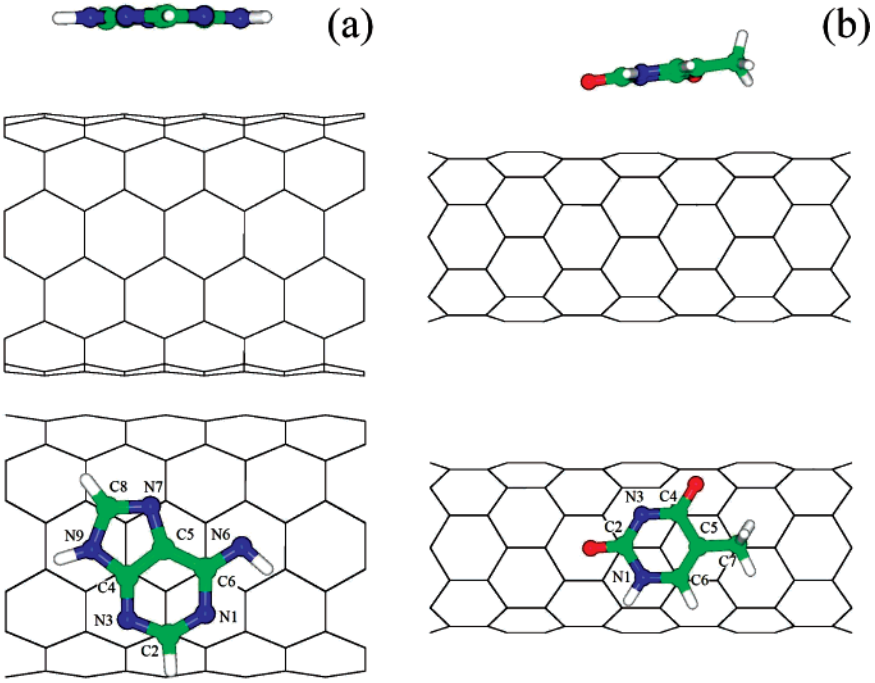

Figure 3. Equilibrium configurations of (a) A-radical on (6,6) SWNT and (b) T-radical on (8,0) SWNT with front and top views, respectively, after relaxation. Each complex is in "Top" configuration.

the T-radical, we also take the most stable configuration from T/SWNT—Top_a. The deprotonated one obtained by the removal of a H atom from N3 is considered here. Such radical has the most stable energy as compared to other deprotonated structures and it can occur in DNA.[32] The T-radical/SWNT is shown on Figure 3b after relaxation. The T-radical is somewhat tilted as compared to T/SWNT with the oxygen opposite to the CH_3 group being closer to the nanotube axis.

To understand better the structural changes in the DNA bases and their radicals involved in the adsorption process, we also calculated their bonds and relative angles before and after adsorption, see Figure 4. There is little change in bond lengths for all molecules. For thymine, adenine, and A-radical there is also little change in the dihedral angles. Thus these compounds stay flat before and after adsorption. Some noticeable changes were found for thymine and T-radical themselves in the dihedral angles. All dihedral angles (their absolute value) for thymine are larger than the dihedral ones for the T-radical with the largest difference of 17° being in the angle N3−C4−C5−C7. This indicates that the T-radical is not flat and it has a "bent" form. After adsorption, however, the dihedral angles for the T-radical become very close to the ones for thymine and the molecule stays essentially flat, but it is tilted with respect to the nanotube axis.

The adsorption energies and equilibrium distances after relaxation are given in Table 1. The data indicate that many local minima for the adsorption of thymine and adenine are possible on the carbon nanotube surface. This is in agreement with previous results for the adsorption of benzene aromatics on nanotubes which showed that the adhesion energy is very shallow and there are several local equilibrium positions.[37−39,47] The values of the adsorption energies and distances for adenine and thymine are consistent with a physisorption process where no chemical bond is formed between the two species.

The largest adsorption energy obtained here for Adenine/SWNT is 0.354 eV with a distance 3.14 Å (Top_60b), although the Top_b configuration is just 1 meV below. For Thymine/SWNT, the largest adsorption energy is 0.316 eV with a distance

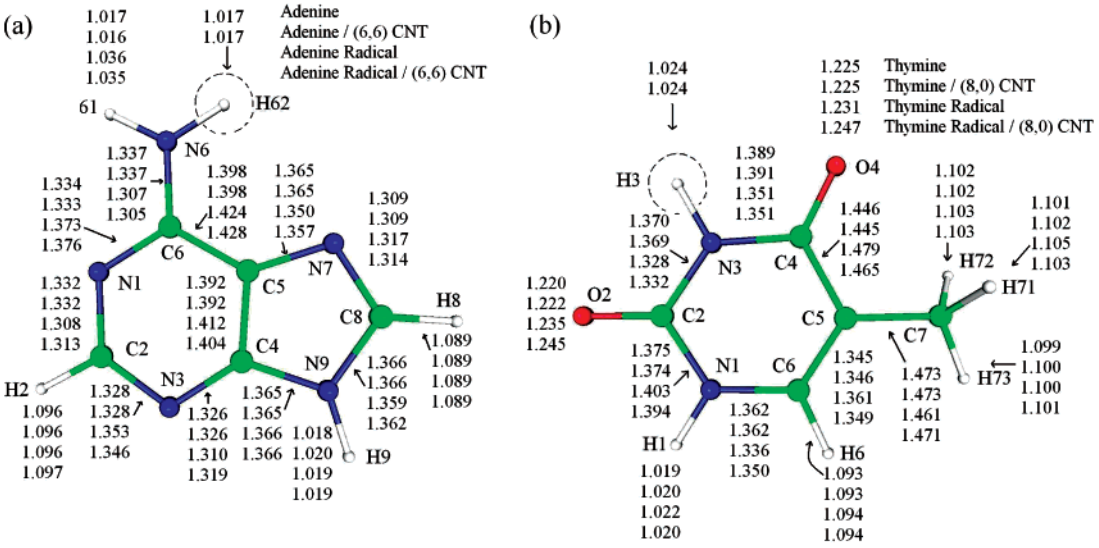

Angle	Thymine	Thymine/ (8,0) CNT	Thymine Radical	Thymine Radical/ (8,0) CNT
A	123.8^0	123.8^0	121.1^0	122.1^0
B	112.7^0	112.8^0	117.5^0	118.0^0
C	128.0^0	127.9^0	125.1^0	122.7^0
D	114.9^0	114.9^0	114.7^0	116.9^0
E	118.1^0	118.0^0	118.4^0	117.3^0
F	122.5^0	122.6^0	120.8^0	120.9^0
G	117.5^0	117.7^0	117.4^0	118.9^0
N1-C6-C5-C7	179.6^0	179.1^0	172.6^0	178.1^0
N3-C4-C5-C7	-179.8^0	-179.2^0	-162.9^0	-177.5^0
C6-N1-C2-O2	180.0^0	178.0^0	-173.7^0	177.5^0
C4-N3-C2-O2	179.8^0	-178.0^0	-174.7^0	-176.6^0
C6-C5-C4-O4	-179.7^0	-178.9^0	-170.6^0	-177.4^0
C2-N3-C4-O4	180.0^0	178.5^0	172.5^0	178.3^0

Angle	Adenine	Adenine/ (6,6) CNT	Adenine Radical	Adenine Radical/ (6,6) CNT
A	119.3^0	119.3^0	120.6^0	120.9^0
B	127.9^0	127.9^0	127.0^0	128.1^0
C	111.8^0	111.6^0	112.4^0	111.6^0
D	126.5^0	126.5^0	126.8^0	127.3^0
E	116.1^0	116.1^0	116.2^0	116.7^0
F	118.3^0	118.4^0	116.3^0	115.4^0
G	122.0^0	122.0^0	122.2^0	122.8^0
H	119.0^0	118.9^0	107.0^0	106.9^0
I	111.3^0	111.3^0	110.5^0	110.4^0
J	104.4^0	104.4^0	104.9^0	105.1^0
K	112.8^0	112.8^0	113.2^0	112.9^0
L	107.1^0	107.1^0	106.5^0	106.7^0
M	104.4^0	104.4^0	104.8^0	104.9^0
N1-C6-C5-N7	-179.2^0	-177.9^0	-180.0^0	-179.0^0
C2-N3-C4-N9	179.3^0	178.1^0	179.9^0	178.9^0
C2-N1-C6-N6	-178.3^0	-178.4^0	-179.5^0	-177.5^0
C4-C5-C6-N6	178.0^0	178.1^0	179.4^0	177.8^0
N3-C4-C5-N7	179.4^0	178.4^0	180.0^0	178.7^0
C6-C5-C4-N9	-178.9^0	-178.0^0	-179.6^0	-179.1^0
C6-C5-N7-C8	178.5^0	177.1^0	179.6^0	178.7^0
N3-C4-N9-C8	-179.3^0	-178.0^0	-180.0^0	-178.6^0

Figure 4. DNA base structures before and after adsorption: (a) bond distance for adenine and A-radical before and after adsorption; (b) bond distance for thymine and T-radical before and after adsorption; (c) angles for thymine and T-radical before and after adsorption; (d) angles for adenine and A-radical before and after adsorption. The dashed circles show the hydrogen atoms removed to form the deprotonated radicals.

3.10 Å (Top_a). We compare these values with the ones reported for the nucleoside/SWNT adsorption (E_{ads} = 0.42−0.46eV).[47] One notes that the adsorption energies calculated here are only about ∼0.1 eV smaller than the ones given in ref 47. The equilibrium distances, however, were found to be of similar magnitude—∼3.10 Å for A and T calculated here and ∼3.3 Å for the nucleoside in ref 47. This indicates that the interaction process is dominated mainly by the base and the rest of components in the larger DNA fragment play a secondary effect.

The adsorption energy and equilibrium distance values we report here are similar to the reported DFT-LDA values for benzene and other simple benzene derivatives, where similar relaxation and convergence criteria were applied.[39] Thus the nitrogenous bases adsorb in a manner similar to that of the benzene derivatives. For the radicals, after the relaxation with spin-polarization was done, we find that the adsorption energies are larger than the ones for the full molecules, see Table 1. The distances are of the same order.

3.2. Electronic Structure. Next we calculate and analyze the electronic structure of the DNA bases and their radicals adsorbed on SWNTs in order to further understand the adsorption process. Figure 5 shows the total electronic density of states (DOS) for the DNA bases and their radicals on the SWNT surfaces. The DOS for the pristine nanotubes is also given as a reference.

TABLE 1: Adsorption Energies and Equilibrium Distances for Adenine and A-Radical on (6,6) SWNT, and Thymine and T-Radical on (8,0) SWNT

configuration	E_{ads} (eV)	D^a (Å)
Adenine/(6,6) SWNT		
Top_a	0.324	3.06
Top_b	0.353	3.05
Top_60a	0.296	3.11
Top_60b	0.354	3.14
Top_90a	0.317	3.10
Top_90b	0.319	3.16
Bridge_a	0.338	3.13
Bridge_b	0.321	3.14
Bridge_30	0.301	3.13
Bridge_60	0.320	3.14
Bridge_90	0.319	3.13
Hollow	0.281	3.25
Hollow_30	0.297	3.24
Hollow_60	0.324	3.21
Hollow_90	0.324	3.19
Thymine/(8,0) SWNT		
Top_a	0.316	3.10
Top_b	0.291	3.16
Bridge_a	0.303	3.11
Bridge_b	0.312	3.22
Hollow	0.247	3.31
Radicals		
A-radical/(6,6) SWNT	0.517	3.14
T-radical/(8,0) SWNT	0.661	2.96

[a] The distances are measured from the center of the hexagonal ring of each molecule to the surface of the nanotube.

First we consider the adsorption of the DNA bases on SWNT. The six-member rings have enhanced stability attributed to the delocalized π electronic structure. The highest occupied molecular orbital (HOMO) for both adenine and thymine is deep in energy and it is completely filled, while the lowest unoccupied molecular orbital (LUMO) for both molecules is completely empty. The band gap of the (8,0) nanotube is not changed and there are no modifications around the Fermi level of the metallic (6,6) nanotube. Thus the electronic transport properties of SWNTs are not expected to change upon adsorption of these DNA bases. The DOS is perturbed at around 1.5 eV under E_F for the (8,0) tube and around 2 eV under E_F for the (6,6) tube. These results are very similar to the total DOS for benzene/SWNT and simple benzene derivative/SWNT upon adsorption[37−39] where no significant changes in the carbon nanotube electronic structure were found due to the benzenes adsorption. Mulliken analysis shows that in both cases there is little charge transfer in the system ≤ 0.01 *e*.

The total DOS for the radicals is also given in Figure 5c and 5f. The spin-polarized calculations indicate that the DOS for both spin species for the A-radical is very similar except for a peak for spin 'down' which appears at the Fermi level of the (6,6) nanotube. This state is mainly of *p* character primarily composed of molecular states and there is very little contribution from the C orbitals from the nanotube. Mulliken analysis shows charge transfer ~ 0.05 *e* in the system. For the T-radical the spin-polarized calculations show that the band gap of the (8,0) nanotube is changed very little and no peaks appear in it. For the spin "down" a peak appears below the top of the valence band composed mainly of *p* molecular states and it does not affect the Fermi level of the nanotube. No such peaks are found for the spin '"up" around the Fermi level. Mulliken analysis gives a charge transfer of ~ 0.03 *e* in the adsorption process.

To gain further insight into the adsorption electronic structure of the radicals for the new features in and around the Fermi level, we give plots of the charge density isosurfaces of four states below the Fermi level, see Figure 6. For T-radical/SWNT, we take the first four states under the Fermi level; for the

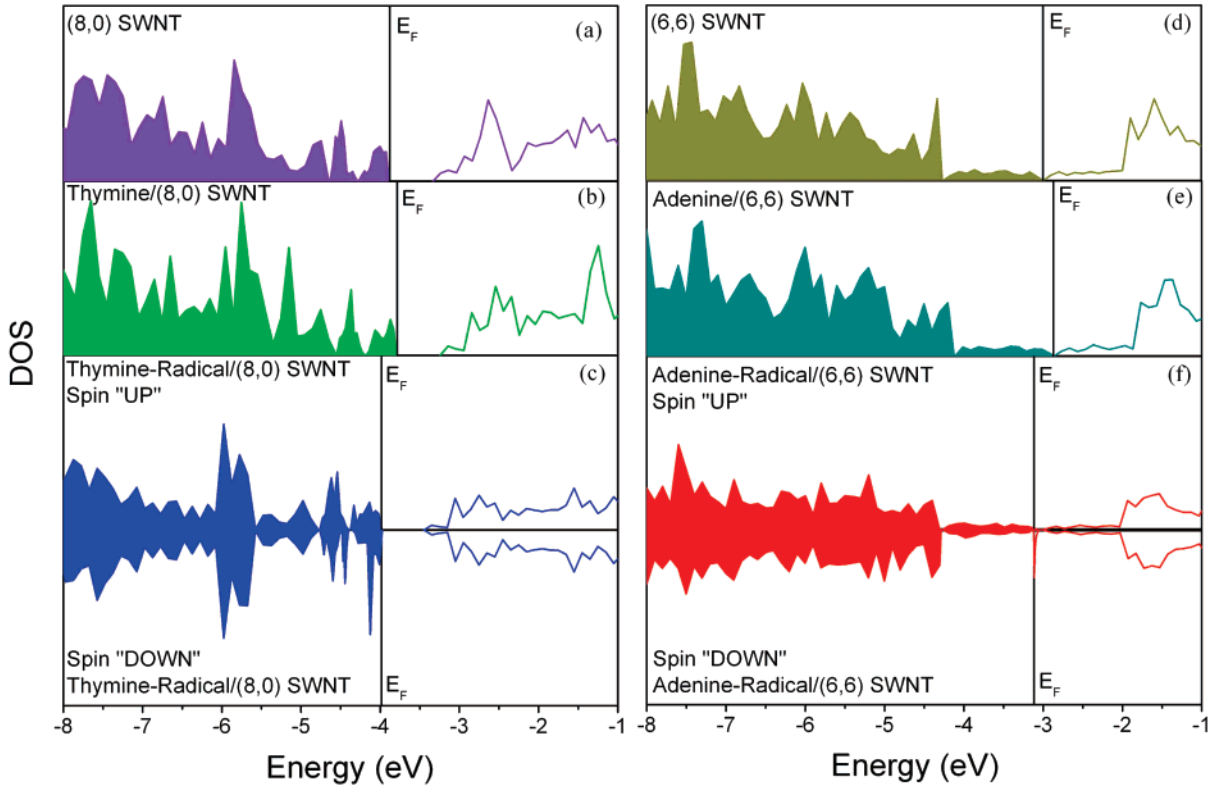

Figure 5. Total density of states for (a) pristine (8,0) SWNT, (b) thymine/(8,0) SWNT, (c) T-radical/(8,0) SWNT, spin-"up", and spin-"down", (d) pristine (6,6) SWNT, (e) adenine/(6,6) SWNT, (f) A-radical/(6,6) SWNT, spin-"up" and spin-"down". For the radicals spin-polarization effects were included in the calculations.

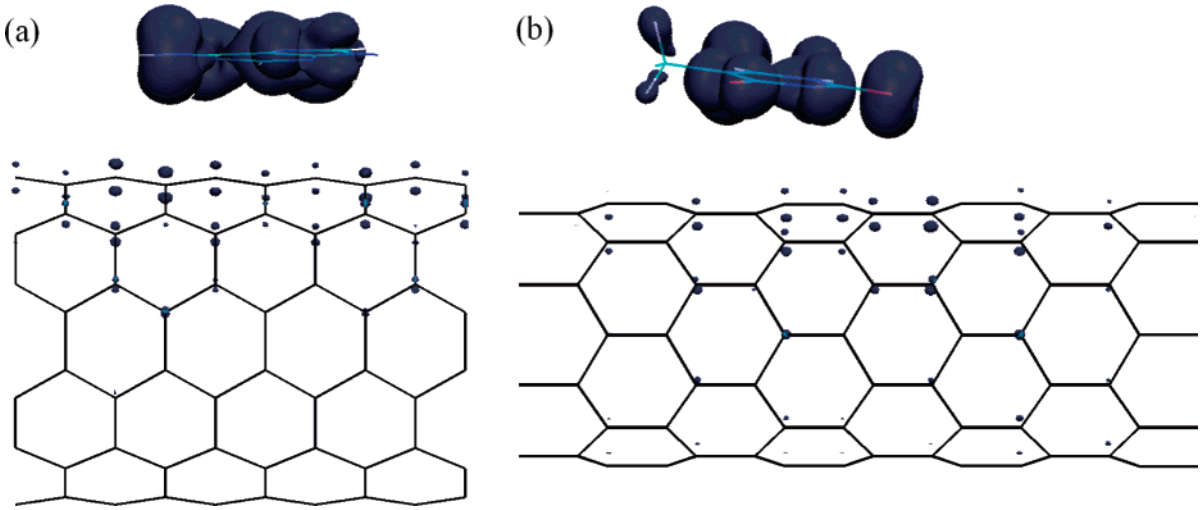

Figure 6. Isodensity surfaces of the charge density for four valence states below Fermi level with isovalue 0.023 $Å^{-3}$ for (a) A-radical/(6,6) SWNT and 0.022 $Å^{-3}$ for (b) T-radical/(8,0) SWNT (created with VMD[49]).

A-radical, we take the state at the Fermi level and the three states right beneath it. For both cases, two of the states are due to the molecule and the other two are due to the nanotube. We find practically no hybridization between the states of the radicals and the highest valence nanotube levels. The adsorption causes some charge redistribution, but mainly within the molecule. This is due to the fact that delocalized π nanotube electronic states are not easily polarized as it was found for the adenine/graphite system.[46] The rehybridization occurs mainly within the surfaces of the radicals.

4. Conclusion

The results from the DFT calculations presented in this work can be used to understand the important factors in the adsorption process of DNA bases and carbon nanotubes. The adsorption of the studied DNA bases and their radicals is of physisorption character. The energies, equilibrium distances, and electronic structure show that the main contribution comes from the noncovalent interaction between the delocalized π-orbitals from the molecules and the nanotubes. We also see that even in the cases of the radicals which have larger electron charge transfer abilities (due to the removal of a hydrogen atom) than the full molecules, the interaction is still physisorption. This is consistent with the adsorption of benzene and benzene derivatives where again the main factor was the $\pi-\pi$ stacking and the effect of the functional groups was only secondary.[37−39] Thus the nitrogenous π-molecules interact in a manner similar to the carbon π-molecules. No significant deformation in the nanotube surfaces and the molecules upon adsorption is seen. The exception is the T-radical which has some "bending" in its shape before adsorption, but after the adsorption it becomes flat.

For the adenine and thymine cases, there is little charge migration between the molecules and the nanotubes. A small charge redistribution is found within the molecules themselves. Analysis of the molecular orbitals shows that they are not changed significantly. This analysis shows the existence of a repulsive Pauli barrier between the π-orbitals of the molecule and the nanotube leading to minimization of the $\pi-\pi$ interaction and determining the equilibrium position of the molecules on the nanotube surfaces in a manner similar to the AB $\pi-\pi$ stacking in graphite. A detailed examination of the contributions to the total energy also shows that the attraction is due mainly to the exchange-correlation interaction which overcomes the repulsive Pauli barrier. Similar results were found for the exchange-correlation energy of adenine adsorbed on graphite.[46] For the radicals, there is some charge transfer to the nanotube although it is still small. Larger charge redistribution within the radicals is seen as compared to the whole molecules. The peaks that appear in the total DOS (right under the band gap for the T-radical/SWNT(8,0) and right at the Fermi level for the A-radical/SWNT(6,6)) are mainly due to the molecular orbitals with very little admixture from the nanotube bands. Again, the attraction is mainly from the exchange-correlation contribution to the total energy.

In summary, our study provides detailed information of the equilibrium distances, adsorption energies, bond changes, charge transfer, and density of states characteristics about the interaction of the smallest π-structure building blocks of DNA. Our results suggest that DNA bases and their radicals can be easily immobilized on nanotube surfaces; DNA bases and their radicals might also be used for noncovalent functionalization of carbon nanotubes.

Acknowledgment. Acknowledgment is made to the donors of The American Chemical Society Petroleum Research Fund for support of this research. We also acknowledge the services of the Research Computing Core at the University of South Florida and the services of the High Performance Computing Facilities of DoD.

References and Notes

(1) Satio, R.; Dresselhause, G.; Dresselhause, M. *Physical Properties of Carbon Nanotubes*; Imperial College Press: London, UK, 2003.

(2) Jensen, A.; Hauptmann, J.; Nygard, J.; Lindelof, P. *Phys. Rev. B* **2005**, *72*, 035419.

(3) Nygard, J.; Cobden, D.; Bockrath, M.; McEuen, P.; Lindelof, P. *Appl. Phys. A* **1999**, *69*, 297.

(4) Chen, R. J.; Zhang, Y.; Wang, D.; Dai, H. *J. Am. Chem. Soc.* **2001**, *123*, 3838.

(5) Wang, X.; Liu, Y.; Qiu, W.; Zhu, D. *J. Mater. Chem.* **2002**, *12*, 1636.

(6) Snow, E. S.; Perkins, F. K.; Houser, E. J.; Badescu, S. C.; Reinecke, T. L. *Science* **2005**, *307*, 1942.

(7) Penza, M.; Antolini, F.; Vittori Antisari, M. *Sens. Actuators, B* **2004**, *100*, 47.

(8) Heller, D. A.; Jeng, E. S.; Yeung, T. K.; Martinez, B. M.; Moll, A. E.; Gastala, J. B.; Strano, M. S. *Science* **2006**, *311*, 508.

(9) Dovbeshko, G.; Repnytska, O.; Obraztsova, E.; Shtogun, Y. *Chem. Phys. Lett.* **2003**, *372*, 432.

(10) Jeng, E. S.; Moll, A. E.; Roy, A. C.; Gastala, J. B.; Strano, M. S. *Nano Lett.* **2006**, *6*, 371.

(11) Li, J.; Tee Ng, H.; Cassell, A.; Fan, W.; Chen, H.; Ye, Q.; Koehne, J.; Han, J.; Meyyappan, M. *Nano Lett.* **2003**, *3*, 597.
(12) Lau, E. Y.; Lightstone, F. C.; Colvin, M. E. *Chem. Phys. Lett.* **2005**, *412*, 82.
(13) Charlie Johnson, A. T.; Staii, C.; Chen, M.; Khamis, S.; Johnson, R.; Klein, M. L.; Gelperin, A. *Semicond. Sci. Technol.* **2006**, *21*, S17.
(14) Tang, X.; Bansaruntip, S.; Nakayama, N.; Yenilmez, E.; Chang, Y.; Wang, Q. *Nano Lett.* **2006**, *6*, 1632.
(15) Chou, S.; Ribeiro, H.; Barros, E.; Santos, A.; Nezich, D.; Samsonidze, Ge.; Fantini, C.; Pimenta, M.; Jorio, A.; Plentz Filho, F.; Dresselhause, M.; Dresselhause, G.; Saito, R.; Zhenh, M.; Onoa, G.; Semke, E.; Swan, A.; Unlu, M.; Goldberg, B. *Chem. Phys. Lett.* **2004**, *397*, 296.
(16) Zheng, M.; Jagota, A.; Strano, M. S.; Santos, A. P.; Barone, P.; Chou, S. G.; Diner, B. A.; Dresselhaus, M. S.; Mclean, R. S.; Onoa, G. B.; Samsonidze, G. G.; Semke, E. D.; Usrey, M.; Walls, D. J. *Science* **2003**, *302*, 1545.
(17) Zheng, M.; Jagota, A.; Semke, E. D.; Diner, B. A.; Mclean, R. S.; Lustig, S. R.; Richardson, R. E.; Tassi, N. G. *Nat. Mater.* **2003**, *2*, 338.
(18) Gao, H.; Kong, Y. *Annu. Rev. Mater. Res.* **2004**, *34*, 123.
(19) Watson. J.; Crick, F. *Nature* **1953**, *171*, 737.
(20) Silaghi, S.; Zahn, D. *Appl. Surf. Sci.* **2006**, *252*, 5462.
(21) Preuss, M.; Schmidt, W.; Bechstedt, F. *Phys. Rev. Lett.* **2005**, *94*, 236102.
(22) Boland, T.; Ratner, B. D. *Langmuir* **1994**, *10*, 3845.
(23) Girifalco, A.; Hodak, M. *Phys. Rev. B* **2002**, *65*, 125404.
(24) Mignon, P.; Loverix, S.; Steyaert, J.; Geerlings, P. *Nucleic Acids Res.* **2005**, *33*, 1779.
(25) Star, A.; Han, T.; Gabriel, J. P.; Bradley, K.; Gruner, G. *Nano Lett.* **2003**, *3*, 1421.
(26) Zhang, J.; Lee, J. K.; Wu, Y.; Murray, R. C. *Nano Lett.* **2003**, *3*, 403.
(27) Gajewski, E.; Dizdaroglu, M. *Biochemistry* **1990**, *29*, 977.
(28) Gohlke, S.; Abdoul-Carime, H.; Illenberger, E. *Chem. Phys. Lett.* **2003**, *380*, 595.
(29) Chen, E. C.; Chen, E. M. *J. Phys. Chem. B* **2000**, *104*, 7835.
(30) Piacenza, M.; Grimme, S. *J. Comput. Chem.* **2003**, *25*, 83.
(31) Evangelista, F.; Paul, A.; Schaefer, H. *J. Phys. Chem. A* **2004**, *108*, 3565.
(32) Profeta, L.; Larkin, J.; Schaefer, H. *Mol. Phys.* **2003**, *101*, 3277.
(33) Kresse, G.; Futhmuller, J. *VASP the GUIDE*, http://cms.mpi.univie.ac.at/vasp/vasp/vasp.html.
(34) Kresse, G.; Joubert, D. *Phys. Rev. B* **1999**, *59*, 1758.
(35) Sinnokrot, M.; Valeev, E.; Sherrill, C. *J. Am. Chem. Soc.* **2002**, *124*, 10887.
(36) Kolmogorov, A.; Crespi, V. *Phys. Rev. B* **2005**, *71*, 235415.
(37) Zhao, J.; Lu, J. P.; Han, J.; Yang, C.-K. *Appl. Phys. Lett.* **2003**, *82*, 3746.
(38) Tournus, F.; Latil, S.; Heggie, M.; Charlier, J. *Phys. Rev B* **2005**, *72*, 075431; Tournus, F.; Charlier, J. *Phys. Rev B* **2005**, *71*, 165421.
(39) Woods, L.; Badescu, S.; Reinecke, T. *Phys. Rev. B* **2007**, *75*, 155415.
(40) London, F. *Z. Phys.* **1930**, *63*, 245.
(41) Fraund, J.; Edelwirth, M.; Krobel, P.; Heckl, W. *Phys. Rev. B* **1997**, *55*, 5394.
(42) Uchihashi, T.; Okada, T.; Sugawara, Y.; Yokoyama, K.; Morita, S. *Phys. Rev. B* **1999**, *60*, 8309.
(43) Freund, J. E. Ph.D. Thesis, Ludwig-Maximilians University, Munchen, 1998.
(44) Komiyama, M.; Uchihashi, T.; Sugawara, Y.; Morita, S. *Surf. Interface Anal.* **2001**, *32*, 53.
(45) Sowerby, S. J.; Petersen, G. B. *J. Electroanal. Chem.* **1997**, *433*, 85.
(46) Ortmann, F.; Schmidt, W.; Bechstedt, F. *Phys. Rev. Lett.* **2005**, *95*, 186101.
(47) Meng, S.; Maragakis, P.; Papaloukas, C.; Kaxiras, E. *Nano Lett.* **2007**, *7*, 45.
(48) Lu, G.; Maragakis, P.; Kaxiras, E. *Nano Lett.* **2005**, *5*, 897.
(49) Humphrey, W.; Dalke, A.; Schulten, K. *J. Mol. Graphics* **1996**, *14*, 33.